SUPPORTING INFORMATION

Advanced density-based methods for the characterization of materials, binding events, and kinetics measurements

Thao P. Doan-Nguyen[a,b] *and Daniel Crespy*[a,b*]

[a] Max Planck-VISTEC Partner Laboratory for Sustainable Materials, Vidyasirimedhi Institute of Science and Technol-ogy (VISTEC), Rayong 21210, Thailand

[b] Department of Materials Science and Engineering, School of Molecular Science and Engineering, Vidyasirimedhi In-stitute of Science and Technology (VISTEC), Rayong 21210, Thailand

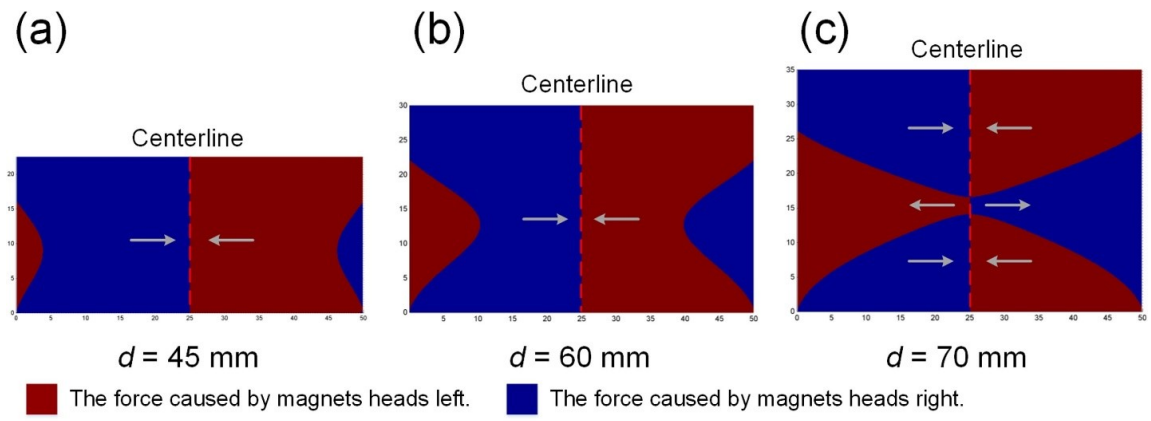

Figure S1. Distribution of the direction of the magnetic force in a horizontal plane in a MagLev containing N45 magnets with dimensions of 50 mm × 50 mm × 25 mm. The distance between the 2 magnets (*d*) was 45, 60 and 70 mm. At *d* = 45 and 60 mm, the magnetic force is directed towards the centerline whereas at *d* = 70, the magnetic force is directed both towards and away the centerline, causing misalignment of the object.[1] Reprinted from ref [1], Copyright (2019), with permission from Elsevier.

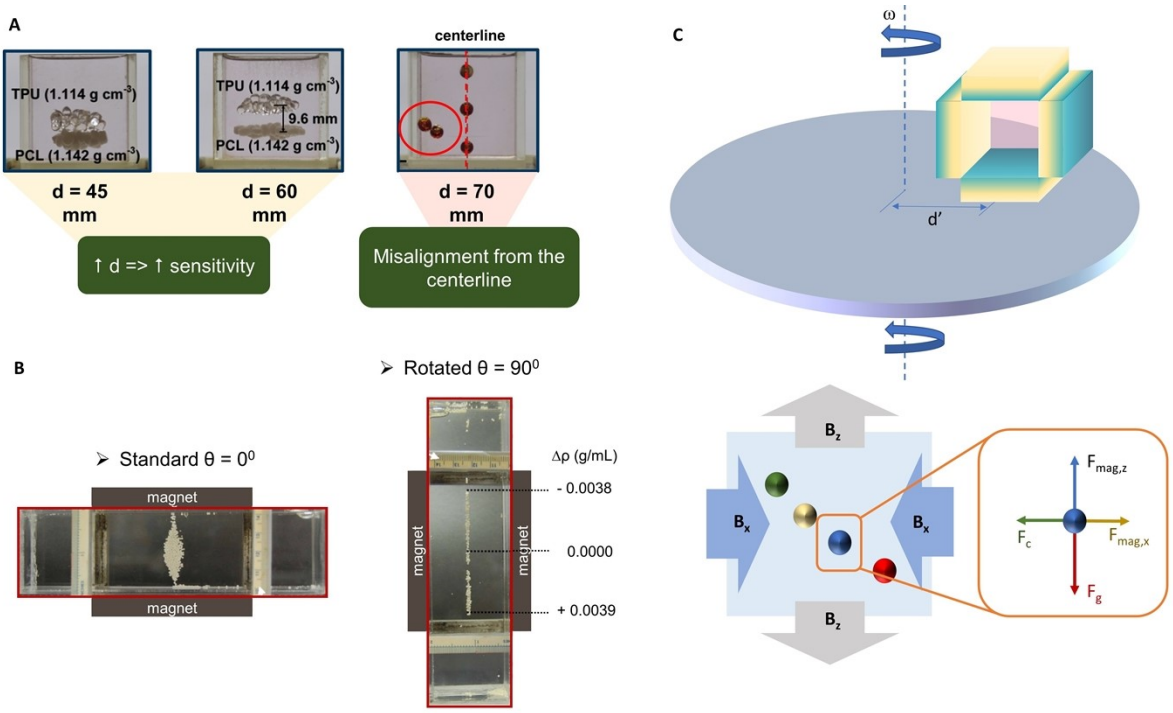

Figure S2. Increasing the sensitivity of MagLev by modifying its configuration. **A.** The difference in levitation heights of thermoplastic polyurethanes (TPU) and polycaprolactone (PCL) was increased when increasing the distance between the two magnets (*d*) from 45 mm to 60 mm (left and middle).[1] Beads were misaligned from the vertical centerline of the two magnets when *d* was increased to 70 mm (right). Adapted from ref [1], Copyright (2019), with permission from Elsevier. **B.** Millimeter-sized drug spheres were analyzed in the standard configuration (left) and rotated configuration of MagLev (θ = 90^0, right).[2] The rotated configuration allowed analyzing spherical drug particles at a higher resolution. Drug particles whose densities were out of the measuring range were separated at the top and bottom part of the cuvette that were not in contact with the magnets. $\Delta\rho$ is the difference between the density of the sample and the medium. Adapted with permission from ref [2]. Copyright 2016 American Chemical Society. **C.** In a centrifugal MagLev, the MagLev device, consisting of 2 pairs of magnets, was placed on a spinning disk.[3] The sample was levitated under the effect of the gravitational force ($\vec{F}_g$), the magnetic force along the x-axis ($\vec{F}_{mag,x}$) and along the z-axis ($\vec{F}_{mag,z}$), and the centrifugation force ($\vec{F}_c$). The sensitivity of the method was tuned by controlling the distance between the MagLev device and the center of the disk (*d'*) and the angular frequency (ω). Adapted from ref [3], Copyright (2019), with permission from Elsevier.

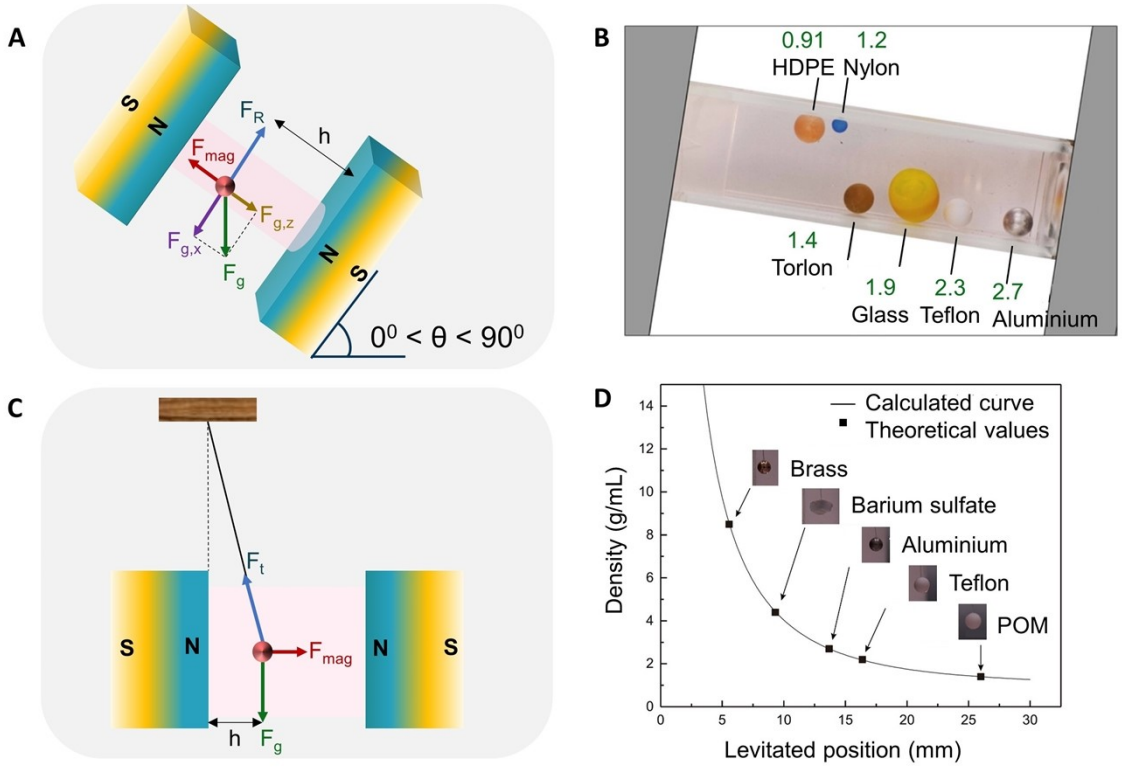

Figure S3. Enlarging the measuring range of MagLev. **A.** When tilting the device at an angle $0^0 < \theta < 90^0$, the gravitational force ($\vec{F}_g$) acting on the object was decomposed into $\vec{F}_{g,x}$ (along the x-axis) and $\vec{F}_{g,z}$ (along the z-axis).[4] $\vec{F}_{g,z}$ was opposed by the magnetic force $\vec{F}_{mag}$ while $\vec{F}_{g,x}$ was opposed by the normal force from the surface of the container $\vec{F}_R$. **B.** Levitation profiles of objects with different densities in a tilted MagLev. The green numbers are densities of the material in g/cm^3. Adapted with permission from ref [4]. Copyright 2016 American Chemical Society. **C.** Horizontal MagLev with the sample attached on a string.[5] The object reached the equilibrium position when the 3 forces: $\vec{F}_g$, $\vec{F}_{mag}$ and the pulling force of the string $\vec{F}_t$ were counterbalanced. **D.** The experimentally measured levitation profiles of different diamagnetic materials attached on a string in a horizontal MagLev were close to-values obtained from the literature. Adapted from ref [5], Copyright (2018), with permission from Elsevier.

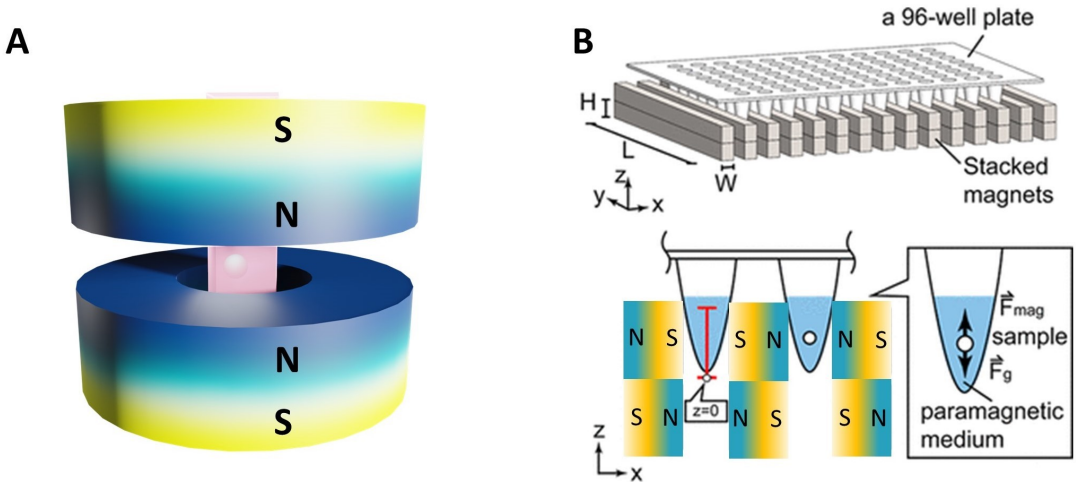

Figure S4. Facilitating the manipulation samples and enhancing throughput can be achieved by changing MagLev configurations. **A.** Axial MagLev with 2 ring magnets.[6] Adapted with permission from ref [6]. Copyright 2018 American Chemical Society. **B.** High-throughput MagLev device.[7] Adapted with permission from ref [7]. Copyright 2018 American Chemical Society.

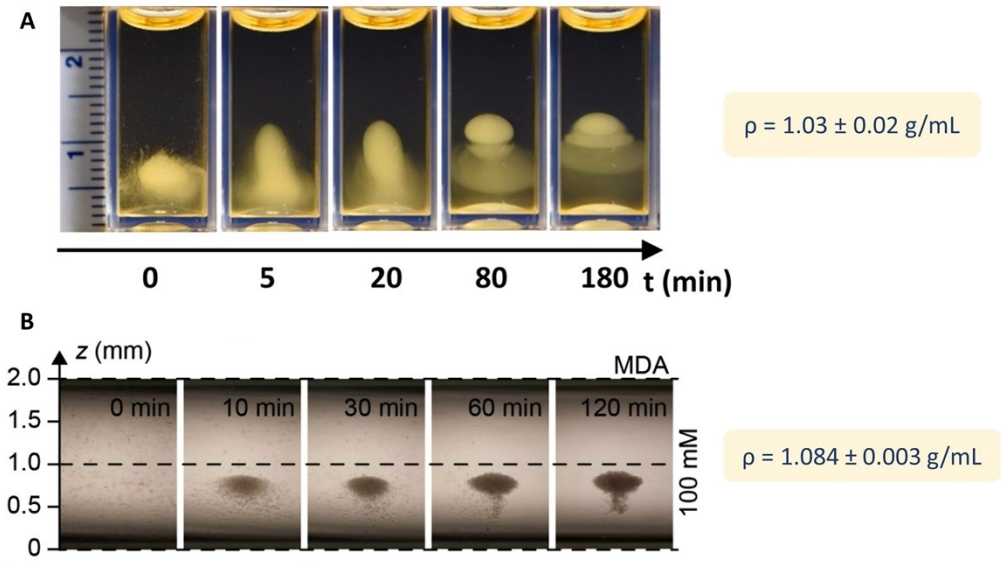

Figure S5. Measuring densities by MagLev of plasma protein[8] (**A**) and human breast cancer cells[9] (**B**) in aqueous dispersions of superparamagnetic iron oxide nanoparticles and aqueous solutions of gadolinium (III) diethylenetriaminepentaacetic acid. A: Reprinted with permission from ref [8]. Copyright 2020 American Chemical Society. B: Reprinted from ref [9], Copyright (2020), with permission from Elsevier.

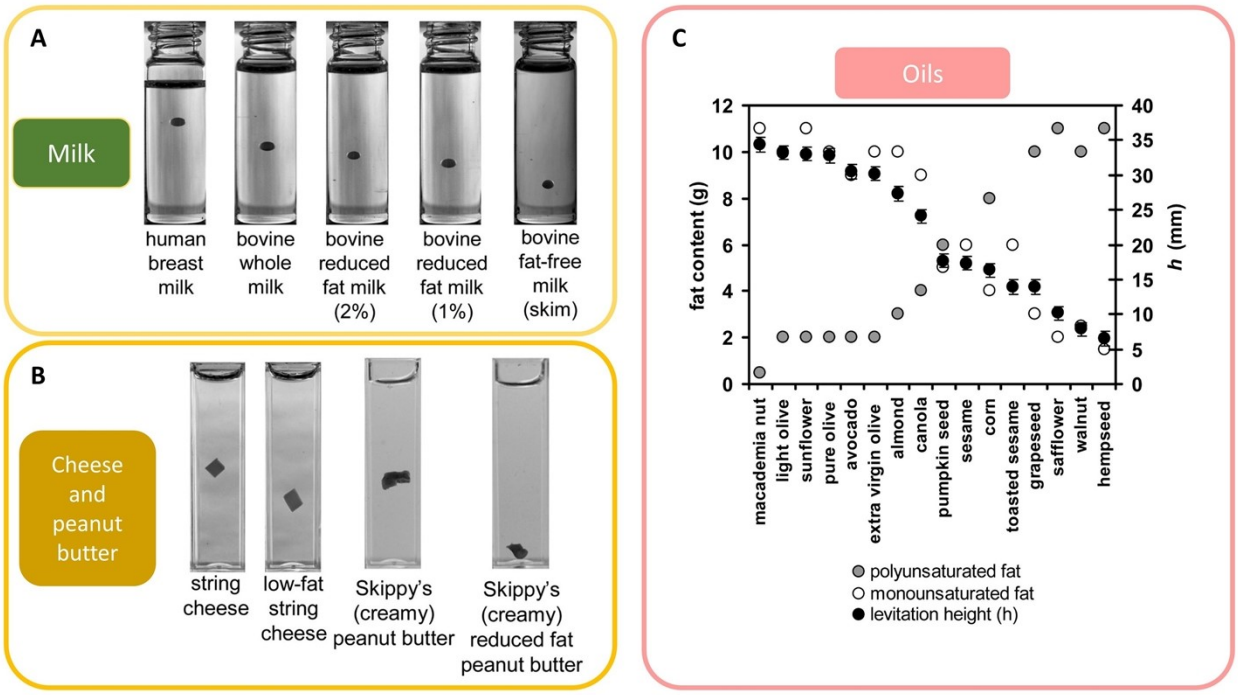

Figure S6. Analyzing the fat content in food using MagLev.[10] **A, B.** Milk, cheese and peanut butter containing high fat displayed higher levitation position than those with low fat content. **C.** Oils containing a high concentration of monounsaturated fat displayed a higher levitation height than those with a high concentration of polyunsaturated fat. Adapted with permission from ref [10]. Copyright 2010 American Chemical Society.

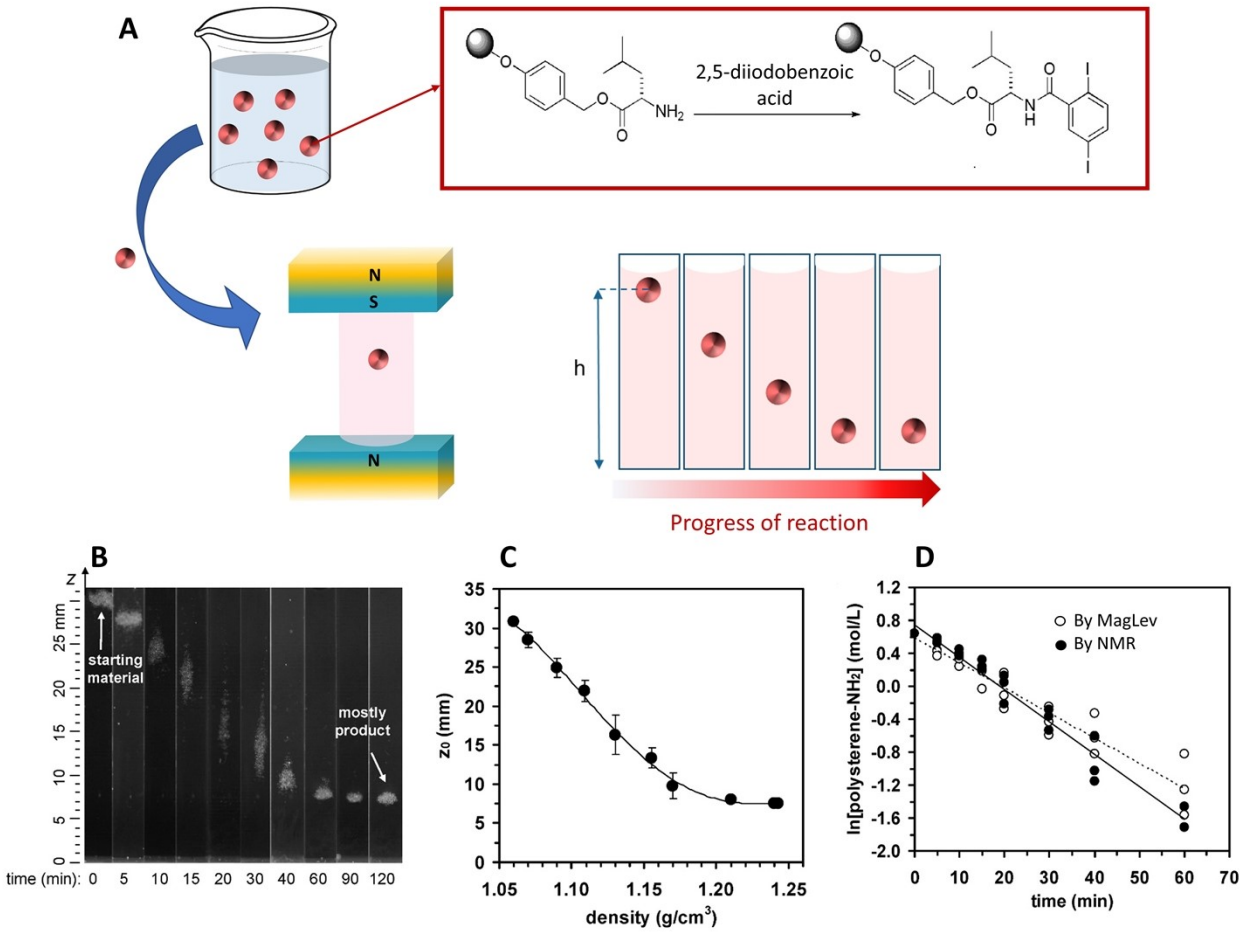

Figure S7. Monitoring a reaction on solid supports by MagLev. The condensation of the carboxyl groups of 2,5-diiodobenzoic acid with the amine groups of leucine coupled on polystyrene beads caused a shift in the levitation height of the beads[11] (**A, B**). The levitation height was used to calculate the density of the reacting mixture (**C**). The concentration of polymer-bound amine measured by MagLev matched the concentration obtained from ^{1}H NMR spectroscopy with a confidence interval of 95% (**D**). Adapted with permission from ref [11]. Copyright 2008 American Chemical Society.

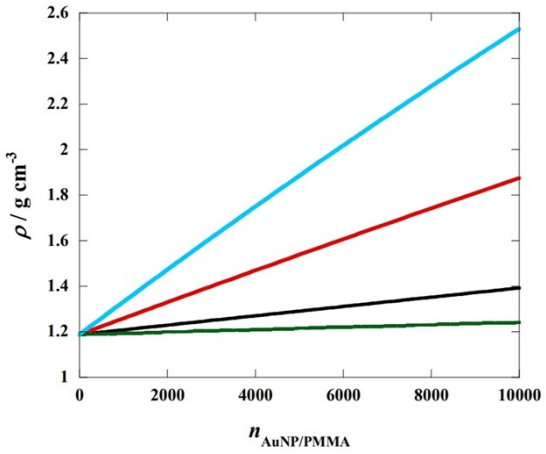

Figure S8. Density of a complex between AuNPs and PMMA microparticle levitated in CAG-field when the number of AuNPs increased from 0 to 10000.[12] PMMA particles displayed different diameters (green: 15 μm, black: 9.57 μm, red: 6.33 μm, blue: 5 μm). The change in levitation coordinate upon binding of AuNPs was more obvious for smaller PMMA particles. Therefore, decreasing microparticle size was useful for increasing the sensitivity of the method. Reprinted with permission from ref [12]. Copyright 2018 American Chemical Society.

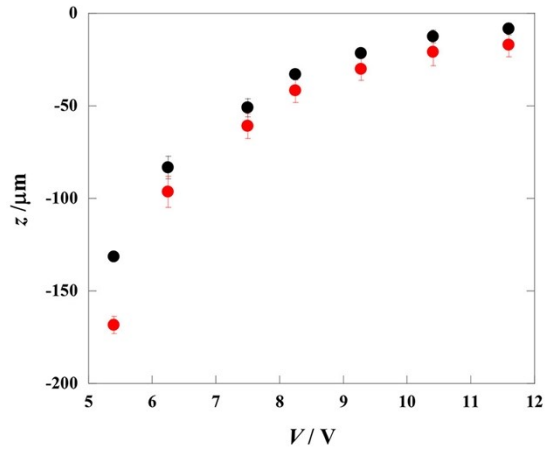

Figure S9. Levitation coordinate of a bare PMMA microparticle (black) and a PMMA microparticle with 10000 AuNPs bound on it (red) when levitated at different voltages in a CAG-field.[12] The levitation coordinate increased when increasing the voltage. The difference in levitation coordinate between bare microparticle and AuNPs-bound microparticle was more obvious at low voltage, hence increasing the sensitivity of the method. Reprinted with permission from ref [12]. Copyright 2018 American Chemical Society.

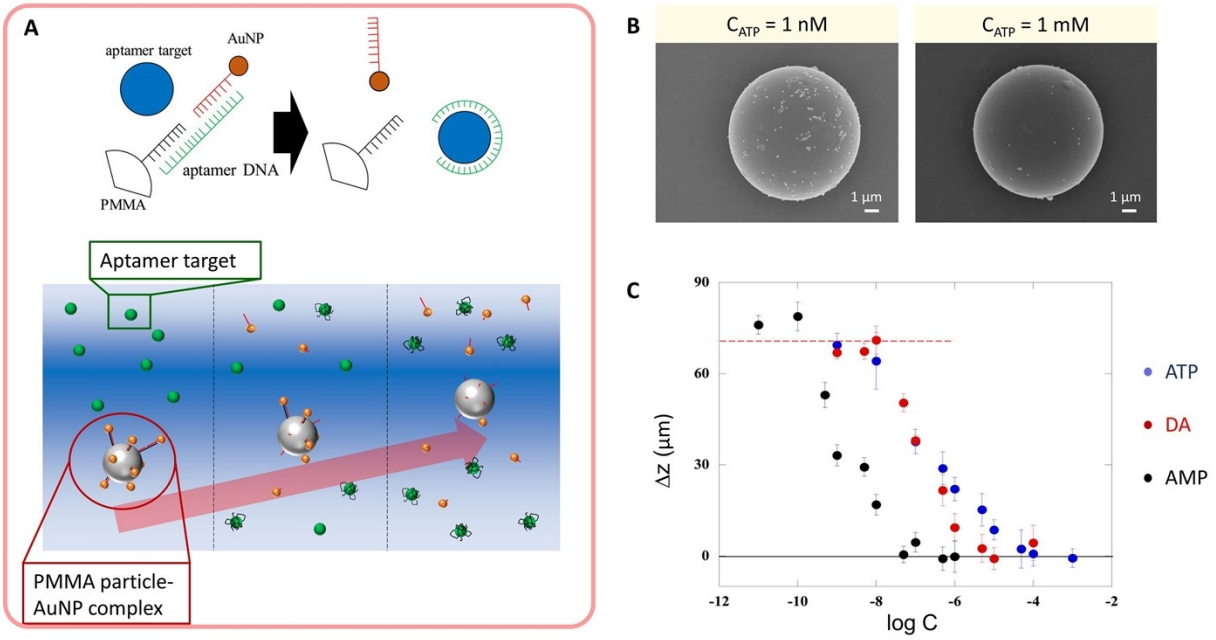

Figure S10. Detecting small molecules by acoustic levitation based on interactions between aptamer DNA and analytes.[13] **A.** Aptamer DNA acted as a bridge to form a binding between a DNA-anchored microparticle and DNA-anchored gold nanoparticles (AuNPs). When the analyte was added, it interacted with the aptamer DNA. The complex between the microparticle and AuNPs was dissociated, leading to a measurable change of the complex's levitation coordinate (Δz). The concentration of the analyte was calculated from Δz. **B.** Micrograph of the complex between AuNPs and a microparticle at different concentrations of the analyte adenosine triphosphate (ATP). **C.** Dependence of Δz on the concentration of different analytes: ATP (blue), dopamine (DA – red), ampicillin (AMP – black).

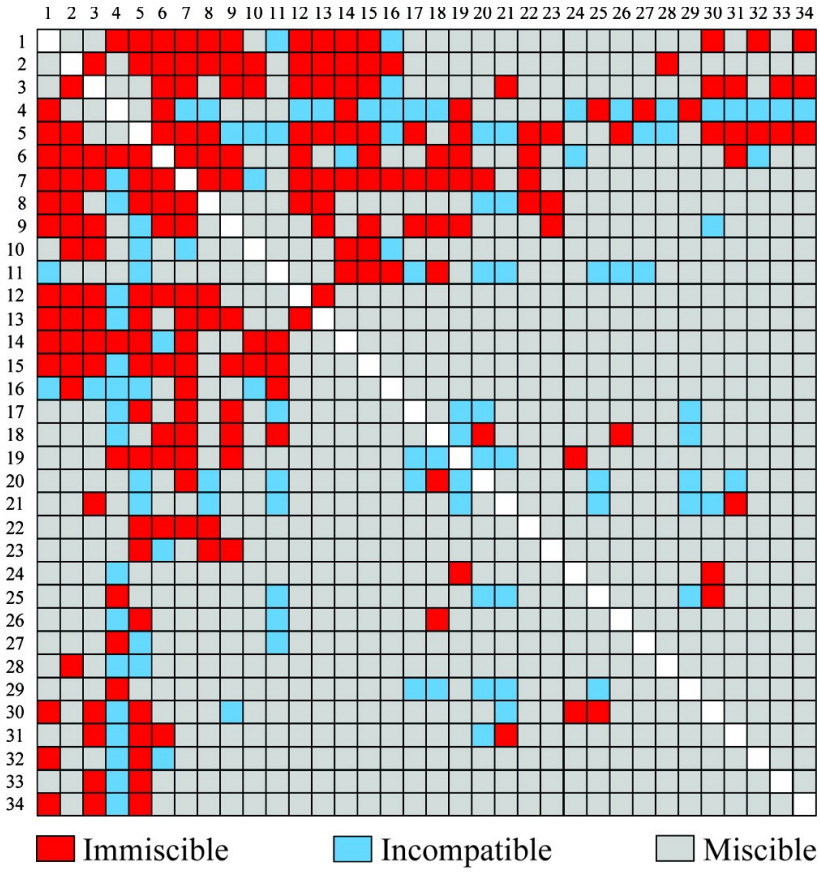

Figure S11. Compositions of aqueous two-phase systems (ATPSs).[14] When mixing solutions of polymers and surfactants, they were either immiscible (red) and formed different phases, or incompatible (blue) – causing precipitation, or miscible (grey). Reprinted with permission from ref [14]. Copyright 2012 American Chemical Society.

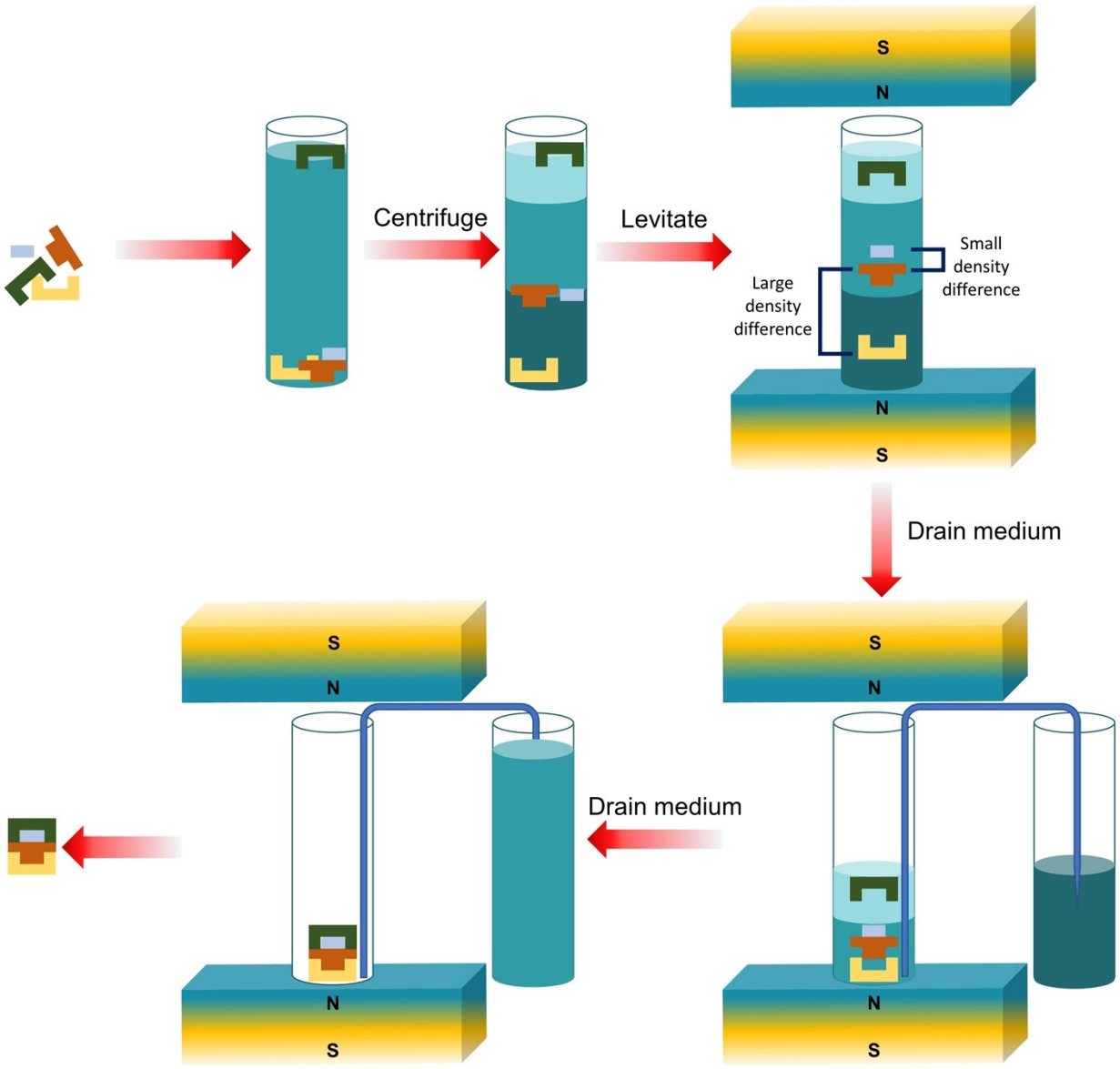

Figure S12. Combination of MuPS and MagLev for the 3D assembly of a mixture of objects displaying various differences of density. The objects are centrifuged with components of a MuPS. Without the presence of the magnetic field, the objects remain at the interfaces of the MuPS. When placed in MagLev, the objects are levitated at different equilibrium positions and align at the vertical centerline of the device. Objects with a large difference in density remain in different phases of the MuPS, while objects with a small difference in density remain at the same phase of the MuPS, but at a different levitation height. Draining the MuPS out of the container promotes stacking of the objects to form a 3D structure.

References

1. Xie, J.; Zhang, C.; Gu, F.; Wang, Y.; Fu, J.; Zhao, P., An accurate and versatile density measurement device: Magnetic levitation. *Sensors and Actuators B: Chemical* **2019,** *295*, 204-214.
2. Nemiroski, A.; Kumar, A. A.; Soh, S.; Harburg, D. V.; Yu, H.-D.; Whitesides, G. M., High-sensitivity measurement of density by magnetic levitation. *Analytical chemistry* **2016,** *88* (5), 2666-2674.
3. Gao, Q.-H.; Li, W.-B.; Zou, H.-X.; Yan, H.; Peng, Z.-K.; Meng, G.; Zhang, W.-M., A centrifugal magnetic levitation approach for high-reliability density measurement. *Sensors and Actuators B: Chemical* **2019,** *287*, 64-70.
4. Nemiroski, A.; Soh, S.; Kwok, S. W.; Yu, H.-D.; Whitesides, G. M., Tilted magnetic levitation enables measurement of the complete range of densities of materials with low magnetic permeability. *Journal of the American Chemical Society* **2016,** *138* (4), 1252-1257.
5. Zhang, C.; Zhao, P.; Xie, J.; Xia, N.; Fu, J., Enlarging density measurement range for polymers by horizontal magneto-Archimedes levitation. *Polymer Testing* **2018,** *67*, 177-182.
6. Ge, S.; Whitesides, G. M., "Axial" magnetic levitation using ring magnets enables simple density-based analysis, separation, and manipulation. *Analytical chemistry* **2018,** *90* (20), 12239-12245.
7. Ge, S.; Wang, Y.; Deshler, N.; Preston, D.; Whitesides, G., High-throughput density-based measurement and separation using magnetic levitation. *Journal of the American Chemical Society* **2018,** *140* (24), 7510-7518.
8. Ashkarran, A. A.; Suslick, K. S.; Mahmoudi, M., Magnetically levitated plasma proteins. *Analytical chemistry* **2020,** *92* (2), 1663-1668.
9. Zhang, C.; Zhao, P.; Tang, D.; Xia, N.; Zhang, X.; Nie, J.; Gu, F.; Zhou, H.; Fu, J., Axial magnetic levitation: A high-sensitive and maneuverable density-based analysis device. *Sensors and Actuators B: Chemical* **2020,** *304*, 127362.
10. Mirica, K. A.; Phillips, S. T.; Mace, C. R.; Whitesides, G. M., Magnetic levitation in the analysis of foods and water. *Journal of agricultural and food chemistry* **2010,** *58* (11), 6565-6569.
11. Mirica, K. A.; Phillips, S. T.; Shevkoplyas, S. S.; Whitesides, G. M., Using magnetic levitation to distinguish atomic-level differences in chemical composition of polymers, and to monitor chemical reactions on solid supports. *Journal of the American Chemical Society* **2008,** *130* (52), 17678-17680.
12. Miyagawa, A.; Harada, M.; Okada, T., Multiple MicroRNA Quantification Based on Acoustic Levitation of Single Microspheres after One-Pot Sandwich Interparticle Hybridizations. *Analytical chemistry* **2018,** *90* (22), 13729-13735.
13. Miyagawa, A.; Okada, Y.; Okada, T., Aptamer-Based Sensing of Small Organic Molecules by Measuring Levitation Coordinate of Single Microsphere in Combined Acoustic–Gravitational Field. *ACS omega* **2020,** *5* (7), 3542-3549.
14. Mace, C. R.; Akbulut, O.; Kumar, A. A.; Shapiro, N. D.; Derda, R.; Patton, M. R.; Whitesides, G. M., Aqueous multiphase systems of polymers and surfactants provide self-assembling step-gradients in density. *Journal of the American Chemical Society* **2012,** *134* (22), 9094-9097.